

PAPER • OPEN ACCESS

## Resistance of magnetic field sensors based on molybdenum nanofilms to intense neutron fluxes

To cite this article: I Bolshakova *et al* 2019 *IOP Conf. Ser.: Mater. Sci. Eng.* **475** 012026

View the [article online](#) for updates and enhancements.



**IOP | ebooks**<sup>TM</sup>

Bringing you innovative digital publishing with leading voices to create your essential collection of books in STEM research.

Start exploring the collection - download the first chapter of every title for free.

# Resistance of magnetic field sensors based on molybdenum nanofilms to intense neutron fluxes

I Bolshakova<sup>1</sup>, M Bulavin<sup>2</sup>, N Kargin<sup>3</sup>, Ya Kost<sup>1</sup>, S Kulikov<sup>2</sup>, M Radishevskiy<sup>1</sup>,  
F Shurygin<sup>1</sup>, M Strikhanov<sup>3</sup>, I Vasil'evskii<sup>3</sup> and A Vasyliiev<sup>1</sup>

<sup>1</sup>Magnetic Sensor Laboratory, Lviv Polytechnic National University

<sup>2</sup>Frank Laboratory of Neutron Physics, Joint Institute for Nuclear Research

<sup>3</sup>Institute of Functional Nuclear Electronics, National Research Nuclear University  
MEPhI

Corresponding author's e-mail address: [inessa@mail.lviv.ua](mailto:inessa@mail.lviv.ua)

**Abstract.** Influence of the reactor neutrons fluxes on parameters of Hall sensors based on molybdenum nanofilms had been investigated experimentally in real-time operation (on-line mode). Sensors sensitivity remained stable up to fluence of  $1 \cdot 10^{24} \text{ n} \cdot \text{m}^{-2}$  at temperature  $\approx 130 \text{ }^\circ\text{C}$ . It allows to recommend molybdenum sensors as the radiation-resistant magnetic diagnostic front-end components for fusion reactors type of ITER and DEMO.

## 1. Introduction

Modern R&D in the field of controlled thermonuclear fusion reached the conceptual design's level of demonstrational fusion reactors, which are called to confirm a viability of electrogenerating systems based on an energy utilization of neutrons and  $\alpha$ -particles produced at the light nuclei coalescence in deuterium-tritium plasma. A flagship project in this direction is the European demonstrational reactor tokamak DEMO that is being developed by the EUROfusion Consortium [1]. A magnetic diagnostics' tools creation is the key task for effective and safety operation of the DEMO type reactors, which could help to resolve the humanity's energy problems and to reduce significantly the adverse impact on ecology already in the 21st century.

It is typical for the deuterium-tritium fusion reactors to have the high radiation (the neutrons, gamma-quanta) and thermal loads within a structure, which lead to characteristics degradation of functional materials used in diagnostic systems. Therefore, the metal inductance coils, which have relatively high tolerance to the radiation and thermal loads, are mainly used as the front-end components (sensors) of magnetic diagnostics. The main disadvantage is that the coils output signal is proportional not to the magnetic induction  $B$ , but to the rate of its change  $\partial B/\partial t$  [2]. So, a coils usage requires the time integration of signal. This leads to errors accumulation due to a number of radiation-induced effects [3]. Nevertheless, the DEMO type reactors are planned to use basically in the steady-state mode when duration of the field pulses' flat-top parts ( $B \approx \text{const}$ ) will be reach hundreds of hours [3]. In this case pick-up coil based systems as reported in [4] become not so applicable. For operation under these conditions it is more appropriate to use the sensors based on Hall effect which can directly measure  $B$  with high precision in the case of both rapid-variable and steady-state magnetic fields.

Earlier the authors of this article have been developed and tested the semiconductor radiation-resistant Hall transducers [5]. In particular, it was confirmed that the sensors based on heterostructures of the In-containing III-V compounds are workable under environment of real fusion reactors (the JET



tokamak, the testing was started on 2009 and continues up today). It was shown experimentally in the research nuclear reactors that they kept a functionality under neutron irradiation up to the limit fluence of  $2 \cdot 10^{22} \text{ n}\cdot\text{m}^{-2}$  [5]. This corresponds to a radiation environment expected at the ex-vessel magnetic field sensors locations in the ITER experimental tokamak throughout its life time ( $\sim 20$  years) [6].

In the next generation fusion reactors of DEMO type the radiation fluxes and neutron fluences at the sensors locations will be hundreds and thousands of times higher than the ITER ones: in the ex-vessel area the fluences will reach  $F \sim (10^{23} - 10^{24}) \text{ n}\cdot\text{m}^{-2}$ , whereas in the in-vessel area it will be  $F \sim (10^{25} - 10^{26}) \text{ n}\cdot\text{m}^{-2}$ . The temperature environment for sensors in DEMO also will be much more rigid: (300 – 500) °C instead of (120 – 250) °C in ITER.

An analysis showed that Hall sensors based on the polycrystalline metal nanofilms can satisfy to these environment. As one of the reasons for their parameters stability under radiation loads it can be considered a presence of the branched network of grain boundaries in material, which are favor a recombination of the interstitial atoms and vacancies formed by the neutron bombardment [7].

At on-line testing in the IBR-2 reactor the authors of this article showed that sensors based on the polycrystalline gold nanofilms demonstrate a high radiation resistance up to fluence  $F \approx 1 \cdot 10^{24} \text{ n}\cdot\text{m}^{-2}$  which was been accumulated for 1852 hours of reactor operation [8]. A character of the sensors sensitivity's dependence on the neutron fluence indicates that reached fluence level is not a limit one for these sensors.

In [9] Hall sensors based on Bi was proposed for ITER. But this metal has low melting temperature  $T_m = 271$  °C, which allows to use it without additional cooling only ex-vessel where the thermal loads in ITER will be  $T \approx 100$  °C, and this is close to the Bi recrystallization temperature  $0.4 \cdot T_m \approx 108$  °C. At the same time in DEMO the working temperatures of the magnetic diagnostics' front-end components expected at the level  $T \approx 200$  °C (ex-vessel, vacuum vessel) and  $T \approx 300$  °C (in-vessel, blanket) [10]. This requires to use the materials with the higher melting temperature  $T_m$  than Bi has.

As a material for Hall sensors in the DEMO environment the molybdenum could be prospective which combines a high melting temperature  $T_m \approx 2617$  °C with a small thermal neutron cross-section  $\sigma \approx 2.6$  barn, which almost 40 times smaller than in Au. In addition, Mo has small linear expansion coefficient, and its Hall coefficient is almost independent on  $T$  in the range  $T = (0 - 600)$  °C [11]. These factors should provide a high stability of Hall sensors based on Mo under the DEMO radiation and thermal loads.

The goal of this work is a radiation resistance testing of Hall sensors based on polycrystalline molybdenum nanofilms under irradiation by reactor neutrons up to the DEMO-relevant fluences.

## 2. Sensors and method of their on-line testing under neutron fluxes

Due to materials activation in consequence of irradiation by neutron fluxes the Hall sensors were tested in the on-line mode that intends a distant automatic parameters measurement with the help of special measuring systems as well as an obtained results transmission onto remote server.

### 2.1. Hall sensors

Investigated samples were manufactured on the basis of polycrystalline Mo nanofilms with a thickness of 50 nm, which were deposited onto  $\text{Al}_2\text{O}_3$  (sapphire) substrate by the vacuum magnetron sputtering method. Ti-based contact metallization is used for both high temperature operation and low sheet resistance of the structure [12]. Identical four-leads Hall sensors in the form of symmetrical crosses with the  $(200 \times 200) \mu\text{m}^2$  active area's dimensions were formed using the lift-off process. The dimensions of separate chip were  $\approx (1 \times 1) \text{ mm}^2$  after dicing. Additional gold contact pads with a thickness of  $(1.5 - 2.0) \mu\text{m}$  was deposited onto sensors leads by the vacuum thermal evaporation method, and the  $\varnothing 30 \mu\text{m}$  gold wires were jointed to them by the thermocompression bonding method to conduct further Hall measurements.

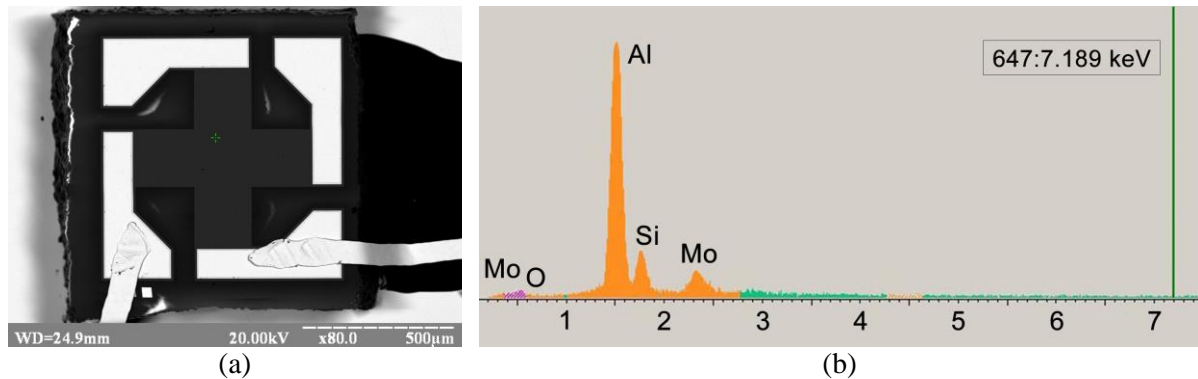


**Figure 1.** The phase-contrast SEM image of the Mo-based Hall sensor with auxiliary wires for the charge removal (a), and the energy-dispersive X-ray spectrum for part of the sensor active area (b).

Figure 1 demonstrates the phase-contrast image of molybdenum Hall sensor (a) and the energy-dispersive X-ray spectrum for part of its active area's surface (b), which were obtained by the PEMMA-102-02 scanning electron microscope (SEM). The presence of Si spike on figure 1 b can be explained by the X-ray photons energy loss on the fluorescence in material of silicon detector.

## 2.2. Measurement of Hall sensors sensitivity

The testing of the Hall sensors radiation resistance in neutron fluxes were carried out by measuring in on-line mode the dependence of their sensitivity  $S$  on fluence  $F$ :

$$S(F) = \frac{1}{I} \cdot \frac{U_H(B, F)}{B}, \quad (1)$$

where  $S$  is the sensitivity,  $I$  – sensor bias current,  $B$  – magnetic induction,  $U_H$  – Hall voltage. Since the samples temperature  $T$  was fixed during on-line testing, its influence does not take into account in (1).

The  $S$  value was defined with taking into account the nonzero parasitic offset voltage  $U_0$  at  $B = 0$  that is adding to  $U_H$ , and, as a result, the sensor output signal is the superposition:

$$U(B, F) = U_H(B, F) + U_0(F), \quad (2)$$

where  $U$  is the output voltage,  $U_0 = U(B = 0)$  – offset voltage.

For the metal sensors  $U_0$  sometimes exceeds  $U_H$  because Hall signal in metals is a very low. Furthermore, the  $U_0$  value can vary significantly for different samples. So, the key task is minimization of  $U_0$  in order to rise a determination accuracy of true Hall voltage  $U_H$ . For that in this work it was used the spinning-current method that intends a quick successive circular synchronous interchanging of the current-leads pair and the voltage-leads pair of the sensor at  $B = \text{const}$  and  $F = \text{const}$  [13]. In so doing an averaging of four  $U$  values measured over one current spinning cycle with duration of  $t_{SC}$  gives the modified output signal that can be expressed as:

$$U^{SC}(B, F) = U_H(B, F) + U_0^{SC}(F), \quad (3)$$

where  $U_0^{SC} \ll U_0$  is the remaining offset voltage. The spinning-current method also allows to reduce essentially a noises and interferences content in output signal, which is especially important at the using of long communication lines during testing in neutron fluxes.

The  $U_0^{SC}$  value can be very low. Modern versions of the spinning-current method allow to reduce the offset voltage by  $U_0/U_0^{SC} \approx 10^4$  times [14]. Nevertheless, at the assessment of a Hall sensors radiation resistance it cannot be assumed that  $U_0^{SC}$  in (3) is equal to zero, because  $U_H$  and  $U_0^{SC}$  are

depend on fluence  $F$  in different ways. Correspondingly for the more precise determination of  $U_H(F)$  and  $S(F)$  it needs to take into account the  $U_0^{SC}(F)$  dependence.

For that purpose in this work the sensors were placed into the periodic pulsed test magnetic field:

$$B = \begin{cases} B_t, & k \cdot P \leq t < (k + D) \cdot P, \\ 0, & (k + D) \cdot P \leq t < (k + 1) \cdot P, \quad k = 0, 1, 2, \dots \end{cases} \quad (4)$$

where  $B_t$  is the test magnetic field amplitude,  $P$  – field pulses period,  $D$  – duty cycle. Demodulation of the output signal obtained in this way allow to separate two components:

$$\begin{aligned} U_1^{SC}(F) &= U^{SC}(B = B_t, F) = U_H(B_t, F) + U_0^{SC}(F), \\ U_2^{SC}(F) &= U^{SC}(B = 0, F) = U_0^{SC}(F), \end{aligned} \quad (5)$$

the difference of which allows to find the Hall voltage:

$$U_H(B_t, F) = U_1^{SC}(F) - U_2^{SC}(F). \quad (6)$$

During on-line testing the sensors bias current was  $I = 40$  mA, the test magnetic field amplitude was  $B_t = 15$  mT, the pulses period was  $P = 4$  min., the duty cycle was  $D = 0.5$ . The one measurement's cycle duration of  $U^{SC}$  by the spinning-current method was  $t_{SC} = 0.1$  sec., which is much less then duration of one field pulse  $P \cdot D = 2$  min. This allowed to do a necessary number of measurements at  $B = \text{const}$ , and to avoid the transient processes that arise at a pulsed field's switching. The initial sensors sensitivity before an irradiation was  $S_0 = S(F = 0) \approx 1.74$  mV·A<sup>-1</sup>·T<sup>-1</sup>.

### 2.3. The testing in neutron fluxes

The radiation resistivity testing of sensors based on the molybdenum nanofilms was conducted in the IBR-2 fast pulsed reactor in the irradiation channel #3 (JINR, Dubna), where the neutron energy spectrum is close to the forecasted one for the DEMO fusion reactor [15]. The general scheme of on-line irradiation experiment is presented on figure 2.

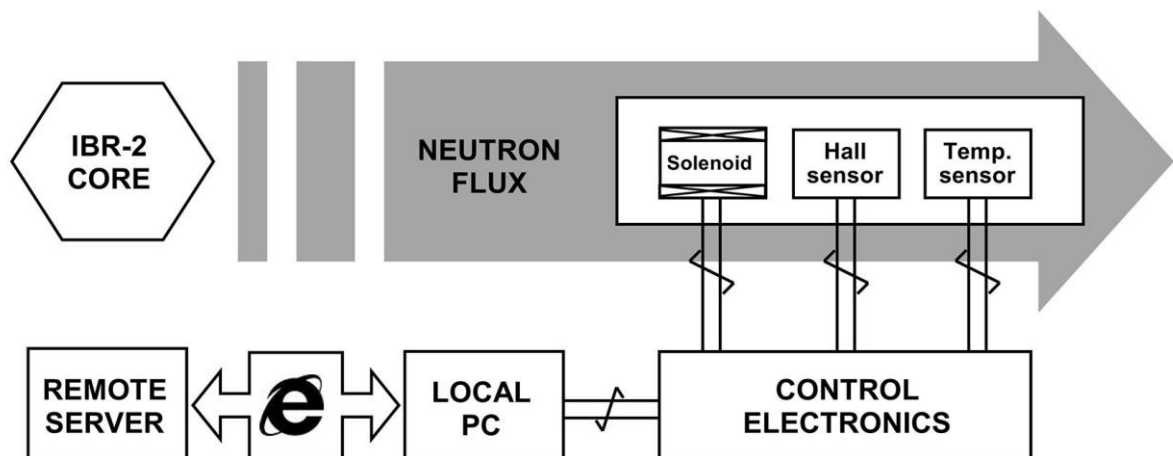


**Figure 2.** The general scheme of on-line experiment on the testing of Hall sensors in neutron fluxes.

The special fixture on the base of radiation- and thermal-resistant ceramics MACOR (Corning, USA) was developed for a samples placement in neutron flux, its elements are presented on figure 3 (a – c). For creation of test magnetic field (4) with  $B_t$  amplitude the  $\varnothing$  10 mm copper solenoid (figure 3 c) was used, inside which the sensors were disposed. The temperature was measured by the platinum resistance thermometer. The fixtures with sensors were mounted into the duralumin

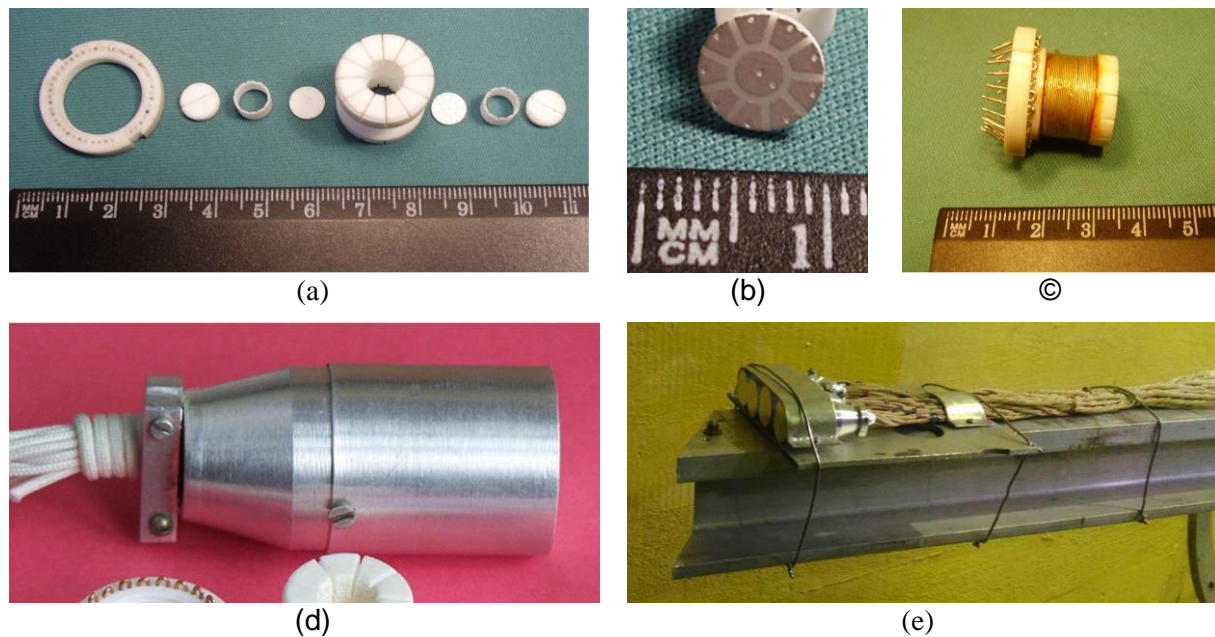


**Figure 3.** The fixture for a samples placement at the testing in neutron fluxes: the structural components (a); the plate for a sensors fixing (b); the solenoid for test magnetic field creation (c); the fixture with sensors inside the duralumin protective screen (d); the fixtures allocation on the supporting beam in the channel #3 of the IBR-2 reactor (e).

protective screens (figure 3 d) and then were fixed on the supporting beam in the irradiation channel (figure e).

For on-line measurements the special highly-sensitive control electronics was developed (figure 2) that realized an algorithm for measurement of small voltage  $U^{SC}$  based on the spinning-current method. This electronics provided the sensors bias current, controlled a solenoid operation, registered the temperature sensor readings, and transmitted obtained data to local PC. The specially designed software performed the  $U^{SC}(F)$  demodulation, separated the  $U_1^{SC}(F)$  and  $U_2^{SC}(F)$  components, and provide their following digital filtering. On the basis of this data it was computed the  $U_H(B = B_r, F)$  dependence adjusted for  $U_0^{SC}(F)$ , as described in subsection 2.2. Obtained results were transmitted to remote server via Internet for the subsequent calculation of  $S(F)$ .

Due to intensive neutron flux the control electronics and local PC were placed outside the irradiation channel – in the IBR-2 reactor hall at a distance of  $\approx 15$  m and in the control room at a distance of  $\approx 40$  m correspondingly. The measuring system components were interconnected by the radiation-resistant cables of the “twisted pair” type (figure 2) in order to reduce an influence of external interferences on measured signals.

During experiment the neutron flux intensity at the location of fixtures with sensors was  $\approx 1.5 \times 10^{17} \text{ n} \cdot \text{m}^{-2} \cdot \text{s}^{-1}$ , which corresponds to the expected in-vessel radiation environment (blanket) in the DEMO reactor [16]. The total irradiation time was 1852 hours, which was allowed to obtain the DEMO-relevant maximum fluence  $F_m \approx 1 \times 10^{24} \text{ n} \cdot \text{m}^{-2}$ .

The samples temperature during experiment was  $T = (130 \pm 5) \text{ }^\circ\text{C}$ .

### 3. Results and discussion

In the result of conducted on-line testing it was obtained about of 45 thousands data points. Figure 4 demonstrates the random sampling from the measured  $S(F)$  dependence. As can be seen the molybdenum sensors in general preserve the sensitivity's stability in the whole considered fluence

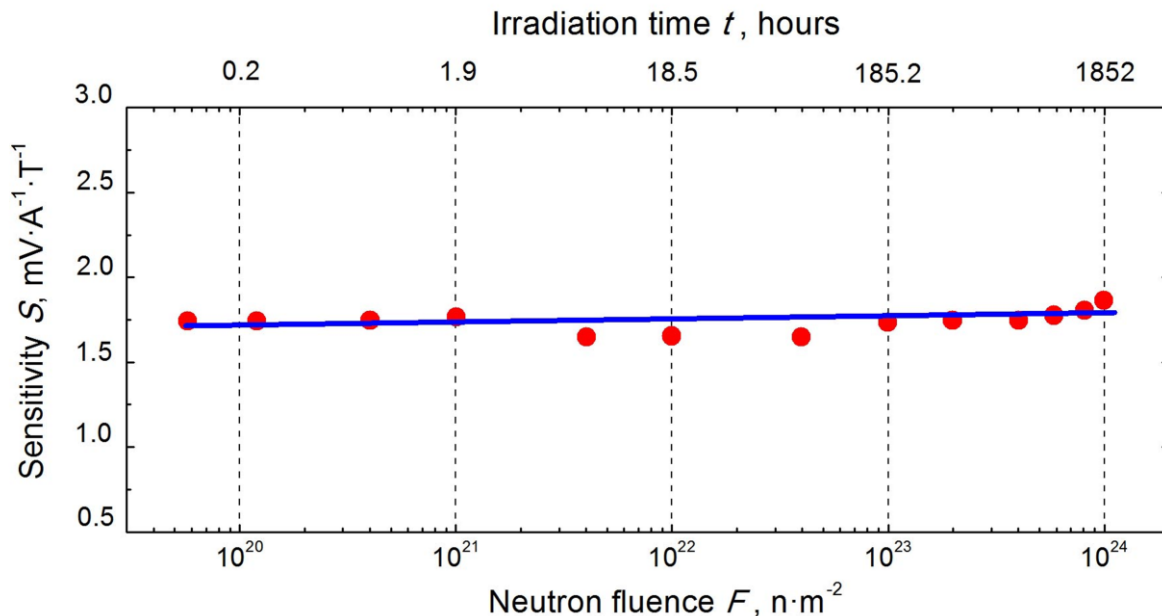


**Figure 4.** The sensitivity dependence on neutron fluence  $S(F)$  (bottom axis) and on irradiation time  $S(t)$  (top axis) for the Hall sensors based on polycrystalline Mo nanofilms: circles mark the measured data, line is the linear approximation.

interval up to maximum value  $F_m \approx 1 \times 10^{24} \text{ n}\cdot\text{m}^{-2}$ . By the end of experiment the relative deviation of  $S$  from the initial value,  $|S(F_m) - S_0|/S_0$ , did not exceed 1 % for all investigated samples. The possible explanation of such high radiation resistance is a presence in the polycrystalline nanofilms of the grain boundaries network, which are favor a recombination of the interstitials and vacancies created under neutron bombardment [7].

The data points rejections from the  $S(F) = S_0$  level on figure 4 can be explained by the operation peculiarities of the IBR-2 reactor (the irradiation sessions are continue 12-15 days with the interruptions form 1 till several weeks) as well as by the insignificant deviations of its output power. This led to the samples temperature changes within  $\pm 5$  °C. Although such  $T$  variations do not affect the Hall voltage  $U_H$  of investigated samples (which is also confirmed by data for Mo obtained in [11]) but they can change the offset voltage  $U_0^{SC}$ . At the same time, it should be noted that the spinning-current method does not remove the offset completely from the measured signal, and consequently the dependence of  $U_0^{SC}$  on  $T$  may reflected to some extent on the results of  $U_H$  measurement. A big problem is the small  $U_H$  value typical for most of metals. As a result at the on-line investigations with the using of long communication lines the electrical noises and interferences become the source of additional inaccuracies of measurement.

An overcoming of these obstacles requires to improve equipment for the metal Hall sensors on-line investigations, in particular that is based on advanced versions of the spinning-current method [14]. Moreover, the improvement of the molybdenum sensors manufacturing technologies is needed to reduce the offset voltage and own noises level, to improve a reproducibility of devices characteristics etc.

#### 4. Conclusions

The sensitivity  $S$  of the Hall sensors based on the polycrystalline Mo nanofilms is stable under an action of reactor neutrons fluxes up to the fluence  $F \approx 1 \times 10^{24} \text{ n}\cdot\text{m}^{-2}$  at the temperature  $T \approx 130$  °C. This confirms the possibility of their using as the ex-vessel front-end components of magnetic diagnostics

for the DEMO type's fusion reactors where the radiation loads  $F \sim (10^{23} - 10^{24}) \text{ n}\cdot\text{m}^{-2}$  are forecasted. The absence on  $S(F)$  dependence of signs of the Mo sensors parameters degradation in the considered fluences  $F$  range allows to expect that the sensors sensitivity will not change significantly at the higher fluences up to  $F \sim (10^{25} - 10^{26}) \text{ n}\cdot\text{m}^{-2}$  typical for the in-vessel magnetic field sensors' positions in DEMO. Nevertheless, the testing continuation is needed to experimentally confirm the Mo sensors radiation resistance in such environment. Moreover, the assessment of their thermal stability in the DEMO's temperatures range is also needed.

### Acknowledgments

The work had been carried out with the support of the Ministry of Education and Science of Ukraine (DB/RAD Project), the EUROfusion Consortium (WPDC Project), and the Competitiveness Program of the National Research Nuclear University MEPhI. The authors are thankful to Mr. Roman Serkiz (Ivan Franko Lviv National University) for the SEM investigations of samples as well as to Dr. Vincent Mosser (Issy Technology Center, Itron France) for the useful consultations as for the spinning-current method.

### References

- [1] Federici G et al 2016 *Fusion Eng. Design* **109-111** 1464
- [2] Hutchinson I H 2002 *Principles of Plasma Diagnostics* (Cambridge: University Press)
- [3] Orsitto F S et al 2016 *Nucl. Fusion* **56** 026009
- [4] Ma Y, Vayakis G, Begrambekov L B et al 2016 *Fusion Eng. Des.* **112** 594
- [5] Bolshakova I et al 2015 *Nucl. Fusion* **55** 083006
- [6] Loughlin M J 2008 IDM number iter\_d\_2f6s7y
- [7] Ackland G 2010 *Science* **327** 1587
- [8] Bolshakova I et al 2017 *Nucl. Fusion* **57** (In press, DOI: 10.1088/1741-4326/aa7867)
- [9] Kocan M et al 2017 *Fusion Eng. Des.* (In press, DOI: 10.1016/j.fusengdes.2017.03.043)
- [10] Koncara B, Draksler M, Costa Garrido O and Meszaros B 2017 *Fusion Eng. Des.* (In press, DOI: 10.1016/j.fusengdes.2017.03.134)
- [11] Frank V 1959 *Appl. Sci. Res.* **B7** 41
- [12] Shostachenko S A, Zakharchenko R V, Ryzhuk R V et al 2016 *Proc. SPIE, International Conference on Micro- and Nano-Electronics* (doi:10.1117/12.2267053)
- [13] Popovic R S 2004 *Hall effect devices* (Bristol and Philadelphia: IOP Publishing)
- [14] Mosser V, Matringe N and Haddab Y 2017 *IEEE T. Instrum. Meas.* **66** 637
- [15] Shabalin E P, Verkhoglyadov A E, Bulavin M V et al 2015 *Phys. Part. Nuclei. Lett.* **12** 336
- [16] Gilbert M R, Eade T, Bachmann C, Fischer U and Taylor N P 2017 *Nucl. Fusion* **57** 046015